Jamming and Flow of Random-Close-Packed Spherical Bubbles: An Analogy with Granular Materials

Rémi Lespiat,[1] Sylvie Cohen-Addad,[2,1] and Reinhard Höhler[2,1]

[1]*Université Paris-Est, LPMDI FRE 3300 CNRS, 5 bd Descartes, 77454 Marne-la-Vallée, France*

[2]*Université Paris 6, UMR 7588 CNRS-UPMC, INSP, 4 place Jussieu, 75252 Paris Cedex 05, France*

(Received 25 January 2010; revised manuscript received 25 December 2010; published 8 April 2011)

Wet foams are random-close-packed assemblies of approximately spherical gas bubbles in a liquid. We report rheological experiments with this material, showing that even though the stiffness and frictional interactions of bubbles strongly distinguish them from solid spherical grains, jamming and flow of wet foams and granular materials are governed by closely analogous laws.

DOI: 10.1103/PhysRevLett.106.148302 PACS numbers: 82.70.Rr, 47.57.Qk, 83.80.Fg

The collective mechanical response of close-packed spherical bubbles, droplets, or grains can be either solidlike or liquidlike [1–4]: When a shear stress σ larger than the yield stress σ_y is applied, the material flows due to local rearrangements in the packing. The dependency of σ_y on packing fraction ϕ has been represented in a generic jamming phase diagram [5], and it has been suggested that the jamming and flow behavior of the materials considered here could be governed by analogous laws and mechanisms [5,6]. We report an experimental test of this conjecture, focused on the rheological behavior of foams and granular materials in a region of the jamming diagram close to a point called J [7,8], where ϕ approaches the random close-packing fraction $\phi_c \cong 0.64$ [9] and where σ_y goes to zero. To compare foams and granular materials under these conditions, both materials should be probed in the same way, but this is not straightforward: Foams are usually characterized by measuring shear stress versus strain rate at fixed ϕ, and such data are often analyzed in terms of the phenomenological Herschel-Bulkley law [3]. Granular materials subjected to shear strains dilate so that ϕ cannot be maintained constant. Therefore, shear experiments and simulations are generally carried out without a constraint on ϕ but with an imposed confining pressure P [10]. This pressure which enhances contact forces between neighboring grains is created by applying a controlled normal stress. In foams and emulsions, P corresponds to the osmotic pressure $\Pi(\phi)$ which describes how the material resists to the squeezing of the bubbles upon extraction of the foaming liquid at constant gas volume [11].

Experiments and simulations have shown that jamming and flow of granular materials are controlled by a *macroscopic* friction coefficient μ, defined as the ratio of shear stress σ to confining pressure P [2,10]. The control of jamming by μ is evidenced by the existence of an upper bound of the slope angle θ for which a granular pile can be in static equilibrium, called the angle of repose θ^* [10]: Since σ and P are determined by projecting the forces of gravity to the tangential and normal directions of the pile surface, we have $\mu = \tan\theta$, so that θ^* corresponds indeed to a critical macroscopic friction coefficient $\mu^* = \tan\theta^*$. For $\mu > \mu^*$, the flow of granular materials is governed by a constitutive law of the following form [10]:

$$\mu - \mu^* = f(I). \tag{1}$$

The dimensionless shear rate I is the product of the shear rate $\dot{\gamma}$ and the typical duration of a rearrangement, set by the interplay between confining pressure and inertia or viscous friction. f is a function for which empirical expressions have been proposed [12,13]. Both the existence of a nonzero angle of repose and the scaling described by Eq. (1) have been considered as features specific to materials with frictional particle interactions, such as granular matter [2,10]. In the case of foams or emulsions where static friction between neighboring bubbles or droplets does not exist, one might expect that the packing has so many possibilities to relax that the angle of repose θ^* should be zero. However, numerical simulations of closely packed hard spheres without static friction have evidenced small but finite angles of repose [13,14]. This raises the question whether the class of materials where jamming and flow are governed by the ratio σ/P includes even close-packed bubbles.

To provide an answer using conventional rheological measurements of stress versus strain rate, such experiments with foams for different fixed bubble packing fractions ϕ close to ϕ_c would have to be compared to measurements of confinement (or osmotic) pressure P under the same conditions. Rather than following this technically challenging approach, we directly impose a controlled ratio σ/P to foam samples, using a setup analogous to a classical experiment where granular materials flow down an inclined plane [10,12,15]. We study randomly close-packed sheets of bubbles, rising below an immersed inclined plane (cf. Fig. 1). The buoyancy force driving this foam induces shear stress σ and confining pressure P, both depending on liquid density ρ, ϕ, the acceleration due to gravity g, the distance z from the bottom of the foam sheet, and the inclination angle θ:

$$\sigma = \rho\phi g z \sin\theta, \qquad P = \rho\phi g z \cos\theta. \tag{2}$$

Thus, in an inclined plane experiment the ratio σ/P can be imposed by choosing θ. The gas volume fraction ϕ increases slightly with z, beyond its value ϕ_c at $z = 0$, due to the balance between the buoyancy induced confining pressure P and the osmotic pressure $\Pi(\phi)$ [11].

At the beginning of each experiment, we produce almost monodisperse bubbles by injecting nitrogen gas and the foaming solution (pure water, Millipore milli-Q, in which 3% g/g of tetradecyl trimethyl ammonium bromide, Sigma, 99%, No. T4762 are dissolved) into a microfluidic flow focusing device [16]. Gas-liquid interfaces of this solution are known to be mobile [17]. The bubbles are stored in a reservoir at the lower end of an inclined plane immersed in the foaming solution (cf. Fig. 1). Here, the bubbles progressively coarsen, due to diffusive gas transfer among neighbors driven by the Laplace pressure. After 10 min, the polydispersity has reached 10% and the average diameter is 120 μm. We then open a gate to release the bubbles at a controlled rate. The foam produced in this way rises upwards along the plane, between two smooth parallel sidewalls held at a distance of 15 mm (125 bubble diameters). The thickness h of the foam is measured by illuminating its bottom surface with a laser light sheet at grazing incidence. The plane that confines the flow at the top is 10 cm long, transparent, and its surface is smooth so that the motion and structure of the foam in contact with it can be observed. For the range of thicknesses h up to 3 mm used in our experiments, the bubbles are to a good approximation spherical. Two video cameras monitor the bubble shape, packing, and motion at the top surface (in contact with the plate) and at the bottom surface (in contact with the surrounding liquid). Correlating successive images taken by the same camera yields the foam velocities at each of the two surfaces. We have measured these velocities for a fixed coordinate x as a function of y, the horizontal coordinate perpendicular to the direction of flow (cf. Fig. 1). These data show that at a distance of more than 1 mm from the lateral walls, the flow profile is to a good approximation independent of y. Therefore, the lateral boundary conditions have no impact on the velocity data discussed in the following, all measured in the middle between the two sidewalls. Furthermore, we find that for the investigated range of experimental conditions, the flow is stationary: the velocities at two positions at a distance of 5 cm along the x axis are the same within experimental accuracy. Finally, we check experimentally that the viscous shear stress exerted on the foam by the liquid below is negligible compared to the foam shear stress induced by buoyancy, using a method described in [18]. To detect shear flow *inside* the foam, related to a velocity gradient in the z direction (cf. Fig. 1), we determine the difference of the top and bottom speeds of the sample ΔV. The foam gas volume fraction ϕ is determined *in situ* using a conductivity probe: we measure the resistance between two flush mounted electrodes inserted into the inclined plane at a distance of 1.2 mm. To analyze these data, we model the foam as a homogeneous continuum and perform numerical finite element simulations of the conduction, taking into account the conductivity of the liquid below as well as the anomalous packing density of the bubble layer that touches the plane and that we observe directly. We adjust the foam conductivity in the numerical model until the calculated resistance between the electrodes matches the measured one. Using a robust empirical relation [19], we deduce the average gas volume fraction from the bulk foam conductivity divided by the conductivity of the liquid. For a static foam sheet we obtain $\phi = 0.63 \pm 0.01$, very close to ϕ_c. Shear flow in the sample induces a small reduction of ϕ which reaches 0.58 ± 0.01 for the largest investigated θ. This dilatancy effect is consistent with numerical simulations of frictionless granular materials [13].

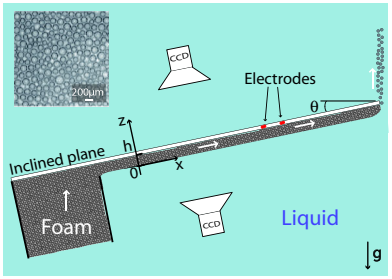

FIG. 1 (color online). Experimental setup. Foam rises below an immersed plane inclined by an angle θ with respect to the horizontal direction. Two CCD cameras monitor the foam speed at the upper and lower foam surfaces. Two electrodes are used to measure the foam's conductivity. The inset shows a typical sample structure.

Figure 2 illustrates our main experimental result: Depending on inclination angle θ and thickness h scaled by the average bubble diameter D, we distinguish solidlike behavior where the foam sheet is translated as a whole ($\Delta V \cong 0$) and liquidlike shear flow where ΔV is larger than 0.35 mm/s, a threshold value chosen close to the experimental limit of detection. Because of the coarsening process, we expect some residual creep flow in the solidlike regime [20] which is, however, beyond our experimental resolution. In the full investigated range of thicknesses h/D, solidlike behavior is observed for an inclination angle below $5.2° \pm 1°$. To refine this estimate of θ^* we plot ΔV versus θ for a fixed foam thickness h (cf. inset of Fig. 2). The velocity difference ΔV remains close to zero in the solidlike regime and it rises sharply with inclination angle in the liquidlike regime. A linear regression of this increase, shown by the straight line, indicates that the angle where ΔV reaches the threshold 0.35 mm/s is typically 0.6° larger than the extrapolated intercept with the abscissa where $\Delta V = 0$. Therefore, the angle of repose is $\theta^* = 4.6° \pm 1°$. This result agrees with two recent numerical simulations, showing a small but finite angle of repose for spherical close-packed particles without any static friction, equal to 3.5° [14] or

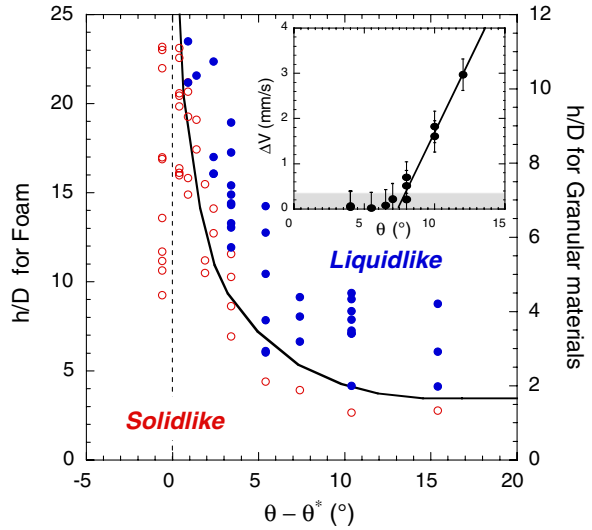

FIG. 2 (color online). Domains of liquidlike (●) and solidlike (○) behaviors, shown as a function of the difference between inclination angle θ and the angle of repose θ^*, as well as h/D. h is the sample thickness and D is the average bubble or grain diameter. The black line is the frontier between the two domains reported for immersed granular materials, made of spherical solid grains of average diameter 112 μm [18]. Data for foams and granular materials, respectively, correspond to the scales shown on the left and right vertical axes. The angle θ^* is 22° for the granular materials [18] and 4.6° for foams, as explained in the text. The inset shows ΔV versus θ for h in the range 1.5 ± 0.2 mm. The region where $\Delta V < 0.35$ mm/s is shaded in gray. The straight line illustrates a linear regression of the data for $\theta > 7.5°$.

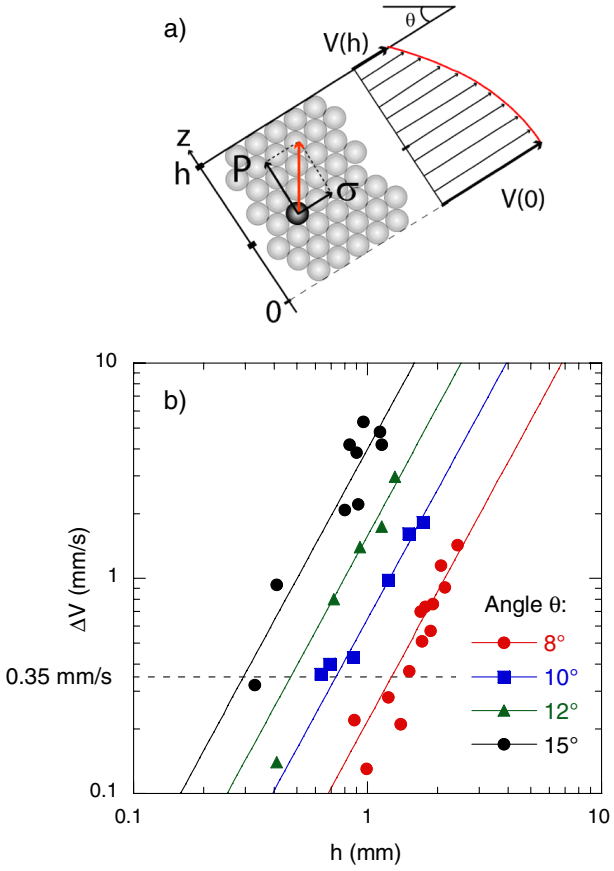

FIG. 3 (color online). (a) Schematic view of the foam flowing below the inclined plane. The foam touches the plane at $z = h$ and the surrounding liquid at $z = 0$. $V(z)$ is the velocity field. (b) $\Delta V = V(0) - V(h)$ measured versus h for different inclination angles. The lines have a slope of 2, predicted by Eq. (3).

$5.76° \pm 0.22°$ [13]. Moreover, the convergence of the measured angle of repose to a constant value for the largest investigated thicknesses h suggests that μ^* is insensitive to the variation of $\phi - \phi_c$ with z. Since μ^* is the ratio of σ and Π under conditions where the sample yields, yield stress and osmotic pressure must scale in a closely similar way with $\phi - \phi_c$ near to the point J. This experimental result agrees with recent numerical simulations of 3D soft sphere assemblies close to the point J [21,22], while two other such simulations, based on 2D assemblies, yield a different scaling behavior [23,24]. Far away from J, μ^* in foams cannot remain independent of $\phi - \phi_c$: For $\phi \to 1$, Π diverges as $(1 - \phi)^{-0.5}$ whereas σ_y goes to a constant value [3,11].

Figure 2 illustrates that the angle of repose converges to the constant θ^* only for $h/D \gg 1$ but that it increases when h/D approaches 1. This finite size effect has been explained by a mesoscopic shear transformation zone model [25]. It is based on the assumption that the probability of a rearrangement is enhanced if other rearrangements have happened in its neighborhood, as also considered in recent models of emulsion fluidity [26]. Close to sample boundaries, the volume of this neighborhood is reduced, so that jamming occurs more easily than in the bulk. Moreover, the characteristic range of interactions between rearrangements is the only independent length scale in this model. A comparison between the finite size effects observed for foams and granular matter suggests that this range decreases with increasing interparticle friction: in Fig. 2 the h/D scale for bubbles is twice that for grains. However, the difference between the smooth boundaries in our experiment and the rough boundary conditions usually chosen in experiments with granular materials could also be relevant.

We now consider the liquidlike regime in detail. To compare our data to Eq. (1), we must first relate I to the experimentally measured quantity ΔV. For flows sufficiently slow so that inertial forces are irrelevant, the time bubbles or grains take to rearrange into a new equilibrium configuration is set by a balance between the confining pressure P and a viscous friction stress that scales with the viscosity η of the liquid in which the bubbles are dispersed. A dimensional argument on this basis yields [18,27] $I = \eta\dot{\gamma}/P$. If we assume that Eq. (1) holds, the choice of an inclination angle θ fixes not only the ratio σ/P but also the value of I. As in previous studies [18], we calculate on this basis the foam velocity profile $V(z)$ by integrating the equation $\dot{\gamma} = IP/\eta$, using Eq. (2), and thus predict the relation between ΔV, h, and I:

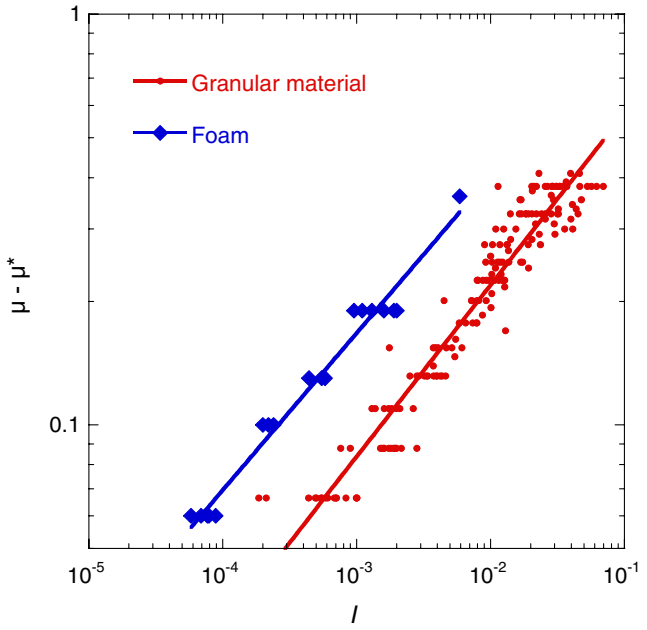

FIG. 4 (color online). Variation of $\mu - \mu^*$, the viscous contribution to the macroscopic friction coefficient, with the dimensionless shear rate $I = \eta\dot{\gamma}/P$ for foams ($\mu^* = \tan 4.6°$) and immersed granular materials ($\mu^* = \tan 22°$) [18]. The foam data are obtained for thicknesses in the range $2.5 < h/D < 24$ and inclination angles $5° < \theta < 20°$. The full lines are power law fits, with exponents 0.38 for foam and 0.42 for immersed granular matter.

$$\Delta V = V(0) - V(z) = \frac{I\rho g\phi\cos\theta}{2\eta}h^2. \qquad (3)$$

Our data shown in Fig. 3(b) agree with the quadratic scaling of ΔV with h predicted by Eq. (3). Moreover, in Fig. 4, we plot $\mu - \mu^*$ versus I, obtained using Eq. (3), and find that for a wide range of angles and sheet thicknesses our foam data collapse on a master plot. These two results validate our assumption that Eq. (1) holds and rule out a dependence of I on h for a fixed angle θ. Remarkably, the master plots for foams and immersed granular materials shown in Fig. 4 are described by power laws whose exponents coincide within experimental accuracy. The prefactors of these power laws and the angles of repose are the only features that distinguish the observed macroscopic mechanical behavior of granular matter and foams for ϕ close to ϕ_c in the investigated range of experimental conditions.

To conclude, our experiments show that jamming and flow of randomly close-packed spherical units can be described in a unified quantitative framework. Assemblies of soft or hard spheres interacting via viscous or solid friction present generic collective mechanical behavior, up to now thought to be specific to granular materials. The similarity between the jamming transition and the glass transition that motivates the term "soft glassy materials" [6] argues in favor of an even larger analogy [28], a challenge that calls for more experiments and new theories.

We acknowledge fruitful discussions with J.-N. Roux, A. Lemaître, and M. Wyart and we thank O. Pouliquen who sent us experimental data for granular materials. J. Laurent, D. Hautemayou, and H. Sizun have provided crucial technical help.

[1] T. G. Mason, J. Bibette, and D. A. Weitz, Phys. Rev. Lett. **75**, 2051 (1995).
[2] P. Jop, Y. Forterre, and O. Pouliquen, Nature (London) **441**, 727 (2006).
[3] R. Höhler and S. Cohen-Addad, J. Phys. Condens. Matter **17**, R1041 (2005).
[4] A. D. Gopal and D. J. Durian, Phys. Rev. Lett. **75**, 2610 (1995).
[5] A. Liu and S. Nagel, Nature (London) **396**, 21 (1998).
[6] P. Sollich, F. Lequeux, P. Hébraud, and M. Cates, Phys. Rev. Lett. **78**, 2020 (1997).
[7] C. S. O'Hern, S. A. Langer, A. J. Liu, and S. R. Nagel, Phys. Rev. Lett. **88**, 075507 (2002).
[8] M. Van Hecke, J. Phys. Condens. Matter **22**, 033101 (2010).
[9] J. G. Berryman, Phys. Rev. A **27**, 1053 (1983).
[10] GDR MiDi Group, Eur. Phys. J. E **14**, 341 (2004).
[11] R. Höhler, Y. Yip Cheung Sang, E. Lorenceau, and S. Cohen-Addad, Langmuir **24**, 418 (2008).
[12] O. Pouliquen, Phys. Fluids **11**, 542 (1999).
[13] P. E. Peyneau and J. N. Roux, Phys. Rev. E **78**, 011307 (2008).
[14] T. Hatano, Phys. Rev. E **75**, 060301(R) (2007).
[15] S. B. Savage, J. Fluid Mech. **92**, 53 (1979).
[16] E. Lorenceau, Y. C. S. Yip, R. Hohler, and S. Cohen-Addad, Phys. Fluids **18**, 097103 (2006).
[17] E. Lorenceau, N. Louvet, F. Rouyer, and O. Pitois, Eur. Phys. J. E **28**, 293 (2009).
[18] C. Cassar, M. Nicolas, and O. Pouliquen, Phys. Fluids **17**, 103301 (2005).
[19] K. Feitosa, S. Marze, A. Saint-Jalmes, and D. J. Durian, J. Phys. Condens. Matter **17**, 6301 (2005).
[20] S. Cohen-Addad, R. Höhler, and Y. Khidas, Phys. Rev. Lett. **93**, 028302 (2004).
[21] T. Hatano, Prog. Theor. Phys. Suppl. **184**, 143 (2010).
[22] M. Otsuki and H. Hayakawa, Phys. Rev. E **80**, 011308 (2009).
[23] P. Olsson and S. Teitel, Phys. Rev. Lett. **99**, 178001 (2007).
[24] B. P. Tighe, E. Woldhuis, J. J. C. Remmers, W. van Saarloos, and M. van Hecke, Phys. Rev. Lett. **105**, 088303 (2010).
[25] A. Lemaître, Phys. Rev. Lett. **89**, 064303 (2002).
[26] J. Goyon, A. Colin, G. Ovarlez, A. Ajdari, and L. Bocquet, Nature (London) **454**, 84 (2008).
[27] P. Rognon, I. Einav, and C. Gay, Phys. Rev. E **81**, 9 (2010).
[28] G. D'Anna and G. Gremaud, Nature (London) **413**, 407 (2001).